ACS APPLIED MATERIALS & INTERFACES

Research Article

www.acsami.org

Robust Mechanical-to-Electrical Energy Conversion from Short-Distance Electrospun Poly(vinylidene fluoride) Fiber Webs

Hao Shao,[†] Jian Fang,[†] Hongxia Wang,[†] Chenhong Lang,[†,‡] and Tong Lin*[,†]

[†]Institute for Frontier Materials, Deakin University, Geelong, Victoria 3216, Australia

[‡]College of Textiles, Donghua University, Shanghai 201620, People's Republic of China

Supporting Information

ABSTRACT: Electrospun polyvinylidene fluoride (PVDF) nanofiber webs have shown great potential in making mechanical-to-electrical energy conversion devices. Previously, polyvinylidene fluoride (PVDF) nanofibers were produced either using near-field electrospinning (spinning distance < 1 cm) or conventional electrospinning (spinning distance > 8 cm). PVDF fibers produced by an electrospinning at a spinning distance between 1 and 8 cm (referred to as "short-distance" electrospinning in this paper) has received little attention. In this study, we have found that PVDF electrospun in such a distance range can still be fibers, although interfiber connection is formed throughout the web. The interconnected PVDF fibers can have a comparable β crystal phase content and mechanical-to-electrical energy conversion property to those produced by conventional electrospinning. However, the interfiber connection was found to considerably stabilize the fibrous structure during repeated compression and decompression for electrical conversion. More interestingly, the short-distance electrospun PVDF fiber webs have higher delamination resistance and tensile strength than those of PVDF nanofiber webs produced by conventional electrospinning. Short-distance electrospun PVDF nanofibers could be more suitable for the development of robust energy harvesters than conventionally electrospun PVDF nanofibers.

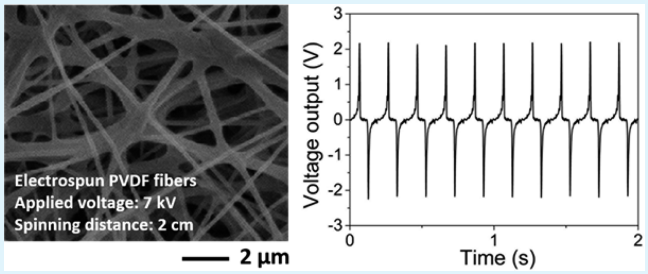

KEYWORDS: *electrospinning, PVDF, interfiber connection, piezoelectric, nanofiber*

INTRODUCTION

Considerable efforts have been devoted to alleviating energy shortage, a global crisis in the coming decades. Apart from upgrading energy technologies, new energy source alternatives are being developed. In particular, obtaining electric power from small mechanical actions has attracted wide interests because small mechanical energies exist widely in our daily life and they are free of concern for the environment.[1−5] Flexible piezoelectric materials with a strong response to small mechanical forces and large electric output are highly desirable.[6]

Polyvinylidene fluoride (PVDF) is a commonly used flexible piezoelectric polymer showing great potential in harvesting small mechanical forces. It has the highest piezoelectric coefficient among flexible piezoelectric polymers. However, PVDF raw material has almost no piezoelectricity due to its nonpolar α crystal phase structure. To attain piezoelectricity, PVDF must be processed conventionally by a program of tedious treatments, including physically stretching and electrically poling under a high electric field at an elevated temperature, to get a β crystal phase of high content and orientated dipoles in the material.[7,8]

Recently, our and other research groups' studies have revealed that PVDF nanofibers produced by an electrospinning technique have already had strong piezoelectricity without need for extra stretching and poling; and electrospun PVDF nanofibers under certain deformations can have even higher mechanical-to-electrical energy conversion ability than conventional piezoelectric PVDF films.[9−12] The use of electrospun PVDF nanofibers for harvesting small mechanical energy would not only simplify the material preparation and processing but also improve the response to small mechanical forces considering that nanofibers are much more flexible than thin films.

In the view of technology, electrospinning is a simple but effective method to produce nanofibers. It involves drawing a viscous solution under a strong electric field to form solid nanofibers. Conventionally, electrospinning is conducted at a nozzle-to-collector distance (i.e., spinning distance) typically greater than 8 cm.[13−15] As a special case, electrospinning is also conducted at a spinning distance shorter than 1 cm (also referred to as "near-field electrospinning").

The main difference between conventional electrospinning and near-field electrospinning is that the jet in conventional electrospinning typically undergoes a whipping movement. As a result, fine and dry fibers form before they deposit on the collector electrode. PVDF nanofibers produced by conventional electrospinning often have a high β crystal phase content, and

Received: July 28, 2015
Accepted: September 17, 2015
Published: September 17, 2015

DOI: 10.1021/acsami.5b06863
ACS Appl. Mater. Interfaces 2015, 7, 22551−22557

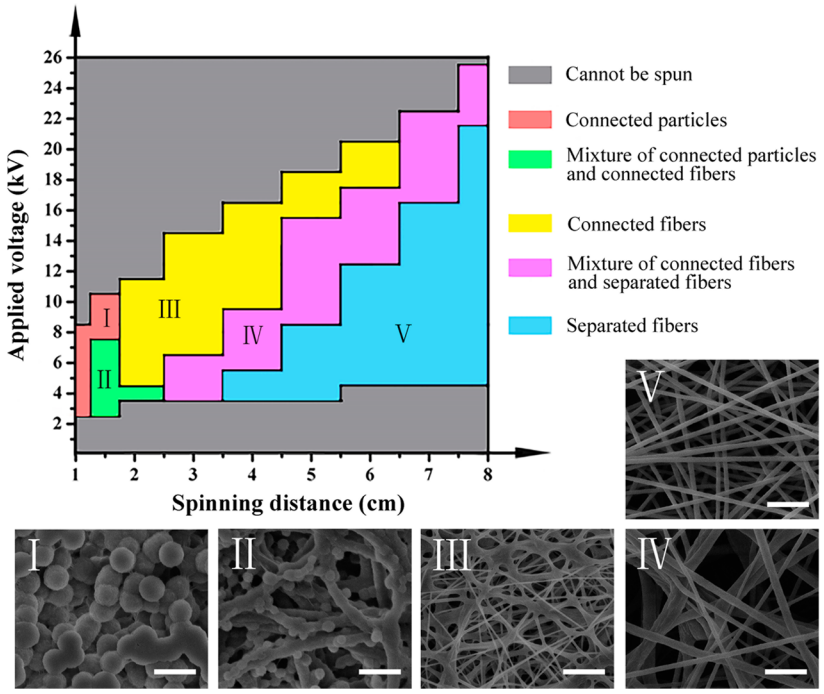

Figure 1. Morphological profile of PVDF electrospun at different parameters. SEM images of different morphology zones: (I) particles, (II) mixture of particles and interconnected fibers, (III) interconnected fibers, (IV) mixture of interconnected fibers and separated fibers, and (V) separated fibers. (Scale bars: 5 μm).

the chain dipole within the nanofibers turns to align across nanofiber web thickness.[10] A PVDF nanofiber web produced by conventional electrospinning can generate an electric output of several volts when it receives a compressive impact.[9] In contrast, no whipping movement takes place for the jet in near-field electrospinning due to the short spinning distance. The macromolecules in near-field electrospun PVDF fibers were reported to align along fiber length.[16] However, single PVDF nanofiber prepared by near-field electrospinning only shows an electrical output in tens of millivolts under bending.[17]

Despite these studies, little attention has been paid toward electrospinning of PVDF nanofibers at a distance between near-field electrospinning and conventional electrospinning. A previous study on electrospinning of PVA has indicated that electrospinning at a spinning distance shorter than 6 cm leads to a macroporous membrane or a dense film attributable to the merging of the highly wet fibers.[18] Wet PVDF fibers should also result when electrospinning a PVDF at such electrospinning conditions. Because wet casting a PVDF solution often leads to a polymer film with α crystal phase,[9,19] it is reasonably expected that electrospun wet PVDF fibers should show low piezoelectricity.

However, our present study has shown that electrospinning at a spinning distance in the range of 1−8 cm (also referred to as "short-distance electrospinning" herein) still results in a fibrous structure except that fibers are highly interconnected. More interestingly, the interconnected PVDF nanofibers have a comparable β crystal phase content and mechanical-to-electrical energy conversion ability to those produced by conventional electrospinning. We have further found that the interfiber connection play a role in stabilizing the fibrous structure during repeated compression/decompression. The short-distance electrospun PVDF nanofiber webs have higher delamination resistance and tensile strength than PVDF nanofiber webs produced by conventional electrospinning. Short-distance electrospun PVDF nanofibers could be more robust for making energy harvesters than conventionally electrospun PVDF nanofibers. Herein, we report our unexpected finding on short-distance electrospun PVDF fibers, and their morphology, crystalline feature, mechanical-to-electrical energy conversion ability, and mechanical properties.

EXPERIMENTAL SECTION

Materials. PVDF pellets (Mw = 275,000), N, N-dimethylformamide (DMF) and acetone were purchased from Sigma-Aldrich, and they were used as received. PVDF pellets were dissolved in the DMF/acetone (4/6 v/v) mixture solvent to prepare a 20% (w/v) solution.

Electrospinning. A purpose-built electrospinning setup was used for electrospinning. The PVDF solution was loaded in a 5 mL plastic syringe capped with a 21G steel needle (inner diameter = 0.8 mm) for electrospinning. The solution flow rate was controlled by a syringe pump (KD Scientific) at 1 mL/h. A high voltage was applied to the needle through a DC power supply (Gamma High Voltage). An aluminum rotating drum (length, 10 cm; diameter, 5 cm; rotating speed: 100 rpm) was grounded and used as the collector.

Characterization. Surface morphology was observed on a scanning electron microscopy (SEM, Joel Neoscope). Fiber diameter was measured based on SEM images using image processing software (ImageJ 1.45s). X-ray diffraction (XRD) patterns were recorded on a Panalytical X-ray diffractometer using Cu radiation of 1.54 Å. The samples were scanned in the 2θ range of 5−30° with a step size of 0.05°. Fourier transform infrared (FTIR) spectra were obtained using a Bruker Optics spectroscopy in attenuated total reflectance (ATR) mode. Differential scanning calorimetry (DSC, TA Q200) was performed in a temperature range of 30−200 °C at the heating rate of 10 °C/min in nitrogen atmosphere. Tensile property of nanofiber webs was tested on Instron UTM (5967) with a crosshead speed of 10 mm/min at room temperature. Up to three specimens for each sample were tested. The strength of the fiber webs at the axial direction was also performed on Instron using double faced adhesive tape at the different stretching speed. The preload was controlled at -2.5×10^{-4} MPa. Mechanical-to-electrical energy conversion property was characterized on an electrochemistry working station (e-Corder 401)

DOI: 10.1021/acsami.5b06863
ACS Appl. Mater. Interfaces 2015, 7, 22551−22557

and a low-noise current preamplifier (Model SR570, Stanford Research Systems). The compression impact was set at a peak force of 10.0 N and frequency of 5 Hz, expect for the experiment of investigating relationship between applied stress and outputs, in which different forces from 0.5 to 15.0 N were applied.

RESULTS AND DISCUSSION

Figure 1 shows the morphology profile of PVDF electrospun at different parameters. When electrospinning the same PVDF solution using different applied voltages and spinning distances, the resulting PVDF could show different morphologies. The two gray zones in the chart specify the conditions where the solution was unelectrospinningable. In the bottom gray zone, the applied voltage was too low to initiate an electrospinning process, while corona discharge occurred in the top gray zone because the applied voltage was above the breakdown limit. Between the two gray zones, PVDF can be electrospun into three main morphologies: particles (zone I), interconnected fibers (zone III) and separated fibers (zone V). Mixtures of particles with interconnected fibers (zone II) and interconnected fibers with separated fibers (zone IV) were also formed.

When the spinning distance was 1 cm, electrospinning resulted in PVDF particles with an average size of 2.9 μm (Figure 1I). The formation of particles comes from strong Coulomb repulsion within the jet because of the high electrical field intensity (~8 kV/cm). In this case, the solution jet at the needle tip tended to form highly charged droplets.[20] Due to the short traveling distance, a certain amount of solvent remained within the particles, making them bond together on the collector.

When the spinning distance was increased from 1 to 2.5 cm, a mixture of particles with interconnected fibers formed when the applied voltage was below 7 kV. The particles had a size around 1.1 μm, while the fibers had a slightly larger diameter than the particle size. The fiber formation was attributed to the reduced electrostatic repulsion within the solution jet.

When the applied voltage was higher than 4 kV and the spinning distance was longer than 1.75 cm, particle-free fibers resulted. As highlighted in the yellow zone, the fibers are interconnected with each other with a wide diameter distribution (Figure 1III). This can be explained by the insufficient whipping movement and limited solvent evaporation from the jet. Wet fibers deposited on the collector, leading to fiber connection.

The blue zone in Figure 1 represents the conditions leading to separated fibers. The fibers electrospun under such a condition (e.g., applied voltage of 12 kV and spinning distance of 6 cm) were uniform with a similar morphology to these prepared under conventional electrospinning condition (e.g., applied voltage of 15 kV and spinning distance of 15 cm), excepted that the short-distance electrospun fibers were coarser (around 500 nm) than the conventionally electrospun ones (diameter 300 nm; see the SEM image in Figure S1, Supporting Information). It was noted that the average electric field intensity in the short-distance electrospinning (2 kV/cm) was higher than that of the conventional electrospinning (1 kV/cm), the larger fiber diameter for the short-distance electrospun fibers suggests that jet stretching and solvent evaporation in the short-distance electrospinning are insufficient. In between the separated fibers and the interconnected fibers, there are some spinning conditions which lead to a mixture of the two fibers (e.g., the pink zone in Figure 1), and the interconnected fibers always had larger diameter (1.2 μm).

The above results indicate that interconnected PVDF fibers can be prepared by electrospinning a PVDF solution at a short distance (2 cm) under an applied voltage in the range of 5−11 kV. However, maintaining the applied voltage at 7 kV but changing the spinning distance from 1 to 8 cm during allows electrospinning PVDF into five different morphologies. With those conditions, we further elucidated the effect of applied voltage on the properties of interconnected PVDF fibers, and the effect of PVDF morphology on the properties. These fibers were also compared with those prepared at a conventional electrospinning condition (applied voltage 15 kV, spinning distance 15 cm). Our previous research revealed that PVDF nanofibers electrospun at this condition (PVDF concentration 20 w/v%) showed optimal mechanical-to-electrical energy conversion property.[12]

Figure 2a shows the XRD patterns of the interconnected PVDF fibers electrospun at different applied voltages (spinning

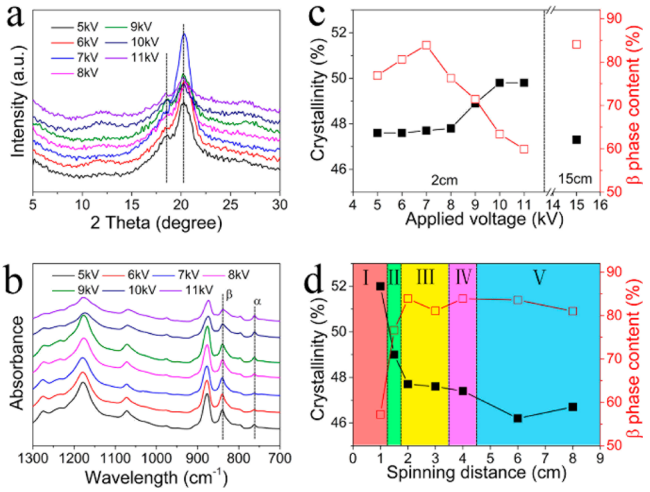

Figure 2. (a) XRD patterns and (b) FTIR spectra of PVDF fibers prepared at different applied voltages (spinning distance 2 cm). Crystallinity and β phase content of PVDF fibers prepared at different (c) applied voltages (spinning distance 2 cm) and (d) spinning distances (applied voltage 7 kV).

distance 2 cm). Two main peaks occurred at 2θ = 18.4 and 20.6, corresponding to the α phase (020) crystal plane and the sum β phase of (110) and (200) planes.[21] The intensity of β crystal phase increased with increasing applied voltage from 5 to 7 kV, and the intensity of α phase decreased accordingly. When the applied voltage was further increased from 7 to 11 kV, the intensity of β crystal phase decreased. To verify the crystal phase structure, we also measured FTIR spectra. As shown in Figure 2b, the characteristic vibration peaks at 840 cm^{-1} (CH_2 rocking) and 1274 cm^{-1} (trans band) are assigned to the β phase.[22,23] Very weak bands at 761 and 976 cm^{-1} attributed to α phase.

It is known that PVDF has five different crystal phases with three different chain conformations: all trans (TTTTT) conformation for β phase, trans−gauche−trans−gauche (TGTG′) for α and δ phases and T3GT3G′ for γ and ε phases.[24] Among them, α and γ phases commonly exist in PVDF, whereas β phase has the highest dipolar moment which plays a significant role in the piezoelectricity.[23]

The β phase content was calculated according to the FTIR result (see the calculation detail in the Supporting Information). As shown in Figure 2c, with increasing applied voltage

DOI: 10.1021/acsami.5b06863
ACS Appl. Mater. Interfaces 2015, 7, 22551−22557

from 5 kV to 7 kV, the β phase content increased from 76.9 to 83.9%. The β phase content gradually decreased to 59.9% when the applied voltage was further increased to 11 kV. This trend can be attributed to two effect factors: electric field and whipping movement. When the voltage was 5 kV, low electric field intensity resulted in coarse fibers with low β phase content (see the fiber diameter distribution in Figure S2). Increasing the applied voltage enhanced the electric field intensity which led to higher electrostatic force to stretch the jet during electrospinning. With increasing the applied voltage from 5 to 7 kV, the average fiber diameter decreased from 1.2 to 0.8 μm. Meanwhile, the β phase content increased. Further increasing the applied voltage to 11 kV caused fiber diameter increase to 2.3 μm and β phase content decrease. At that time, higher applied voltage resulted in higher fiber deposition speed, causing shorter time for whipping movement. More solvent remained in the fibers on the collector. They were easy to collapse to form coarse and oval-shaped fibers, and tended to form more α phase (Figure S2).

Differential scanning calorimetry (DSC) was measured to estimate the crystallinity of the PVDF fibers (see Figure S3). With increasing the applied voltage for electrospinning, the melting endothermic peak of the PVDF shifted to a higher temperature first and then returned to a lower temperature. The fiber crystallinity was calculated and the result was also shown in Figure 2c. The crystallinity in the electrospun PVDF maintained at a constant level when the applied voltage during electrospinning increased from 5 to 8 kV. An obvious increase in the crystallinity occurred when the applied voltage increased from 8 to 11 kV. It was reported that molecular orientation in electrospun fibers was proportional to the degree of crystallinity.[25,26] The increased crystallinity indicates that molecular orientation degree is enhanced by increasing the applied voltage during electrospinning of PVDF fibers at a short distance.

In comparison with the PVDF nanofibers electrospun under the conventional electrospinning condition, short-distance electrospun interconnected PVDF fibers had higher crystallinity but lower β phase content. Only the sample prepared at 7 kV had a comparable β phase content similar to the conventional electrospun nanofibers. Because the crystallinity represents the sum of α and β crystal phase contents in the electrospun fibers, high net β phase content in a material should come from the contribution from both crystallinity and β phase content.

The effect of PVDF morphology on fiber crystal structure and crystallinity was examined. Figure 2d shows the β phase content and crystallinity of PVDF electrospun at 7 kV and spinning distance in the range of 1−8 cm (see the XRD, FTIR, and DSC results in Figures S4−S7). The PVDF particles showed higher crystallinity (52%) but lower β phase content (57.2%) than fibrous PVDF. The high electric field intensity at the short spinning distance may contribute to the higher crystallinity in PVDF particles, meanwhile the low β phase content could be resulted from insufficient stretching during particle formation. When the spinning distance was 2 cm, the electrospun product changed completely to fibers with crystallinity and β phase content of 47.7 and 83.9%, respectively. The interconnected fibers showed higher crystallinity than the separated fibers; however, their β phase content was closed to each other. At the constant applied voltage, increasing the spinning distance reduced the electric field intensity. For this reason, jet at longer distance should receive lower electric field force. On the other hand, increasing the spinning distance offers more time and space for jet to undergo whipping movement, facilitating fiber stretching and solvent evaporation. Therefore, the almost unchanged β phase content with the variation of spinning distance in the range of 2−8 cm stems from the effect of fiber drawing and solvent evaporation during electrospinning.

We evaluated the mechanical-to-electrical energy conversion property of the electrospun PVDF webs by repeatedly compressing and decompressing the PVDF webs. Figure 3a shows the electric outputs of the fiber webs. Under mechanical impact (force of 10 N), the web generated a pulse electric output, while an electric output of opposite polarity formed once the web was decompressed. These output signals are similar to our previous report on randomly orientated electrospun PVDF nanofiber webs.[9]

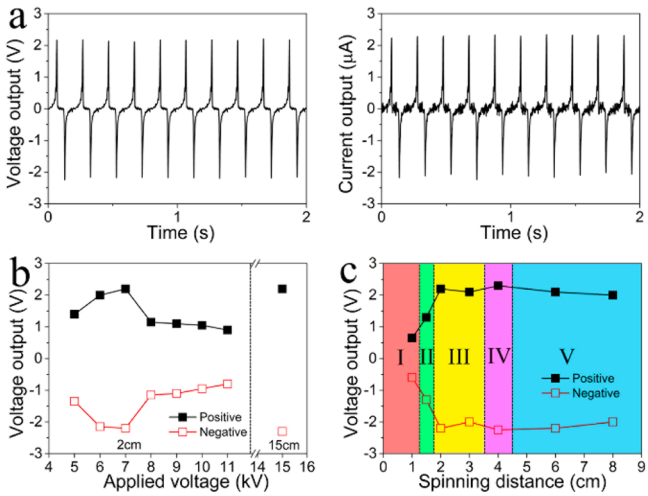

Figure 3. (a) Voltage and current outputs of PVDF fiber web electrospun at 7 kV and 2 cm, (b) peak voltage outputs of PVDF fiber webs prepared at different applied voltages (spinning distance 2 cm), and (c) different spinning distances (applied voltage 7 kV). (Web thickness, 100 μm; working area, 4 cm^2).

It should be noted that compressive stress and strain should have effects on the electric outputs. Increasing the compressive force from 0.5 to 15.0 N led to increase in both voltage and current outputs (see Figure S8), and the electric outputs at low forces followed different trend to those at higher ones. At a force range of 0.5−4.0 N, the voltage and current showed rapid increase with increasing the force, whereas slight increase in electric outputs resulted when the force increased from 4.0 to 15.0 N. This suggests that the fiber web deforms at a low compression, and the larger force causes the elastic deformation of the compressed fibers. However, it was difficult to precisely adjust the strain during measurement due to the thin and flexible features of the PVDF nanofiber webs. Therefore, in the further study, we kept the compression force at 10.0 N to test all nanofiber webs (working area 4 cm^2).

Figure 3b shows the peak voltage outputs of interconnected PVDF fiber webs produced at 2 cm spinning distance and different applied voltages (5−11 kV) (see output signals in Figure S9). For the fiber web prepared at 5 kV, the voltage and current output were 1.40 V and 1.35 μA, respectively. Increasing the applied voltage to 7 kV increased both voltage and current outputs to 2.20 V and 2.30 μA. Further increasing the applied voltage resulted in decrease in electric outputs.

DOI: 10.1021/acsami.5b06863
ACS Appl. Mater. Interfaces 2015, 7, 22551−22557

Table 1 shows the electric output of interconnected PVDF fiber web with different thicknesses (see the corresponding

Table 1. Relationship between Areal Density, Thickness and Electric Output of Fiber Webs

electrospinning parameters		areal density (mg/cm^2)	thickness (μm)	peak voltage (V)	peak current (μA)
short-distance	distance, 2 cm; voltage, 7 kV	1.3	30	1.80	2.00
		2.5	54	2.55	2.90
		3.6	78	2.45	2.65
		4.4	100	2.20	2.30
		6.2	130	1.90	1.90
		13.4	270	0.75	0.85
conventional	distance, 15 cm; voltage, 15 kV	4.4	175	1.55	1.55
		2.7	100	2.25	2.35

voltage and current outputs in Figures S10 and S11). For comparison, the electric output of conventionally electrospun PVDF fiber web with areal densities 2.7 mg/cm^2 (thickness, 100 μm) and 4.4 mg/cm^2 (thickness, 175 μm) were also included in the table. Among the short-distance electrospun fiber webs listed, the highest voltage (2.50 V) and current (2.90 μA) were generated from the sample with an areal density of 2.5 mg/cm^2 (web thickness about 54 μm). At the equivalent areal density, the conventionally electrospun PVDF nanofiber web produced a slightly lower voltage and current outputs.

It was also noted that at the similar areal density level, the short-distance electrospun fiber web was only around half thickness of the conventionally electrospun one due to the larger bulk density. At the same thickness (e.g., 100 μm), the conventionally electrospun PVDF nanofiber web showed a similar electric output to the short-distance electrospun PVDF fiber webs.

The excellent mechanical-to-electrical energy conversion properties of the short-distance electrospun interconnected PVDF fiber web can be explained by two reasons: (1) the dense fibrous structure facilitates charge transfer across the web and hence decreasing the internal resistance, and (2) the fiber−fiber interconnection assists in charge transfer because it eliminates the boundary. These allow the interconnected fiber webs more efficient in the energy conversion than separated fiber ones.

Figure 3c shows the peak voltage outputs of PVDF with different morphologies (see output signals in Figure S12). The lowest electric outputs were recorded on the PVDF particle film (0.75 V and 0.70 μA). The fibrous PVDF (from zones III−V) showed considerably higher electric output than PVDF particle film. The voltage output showed a similar trend to β phase content. This indicates that β phase in the electrospun product play a critical role in deciding the electric output, which was in accordance to our previous report on PVDF nanofibers produced by conventional electrospinning.[12]

Another advantage of fiber-interconnection is the ability to maintain structure integration. Figure 4 shows a series of photos taken during fast compression and decompression of a PVDF fiber web. For the web made of separated fibers which are prepared by conventional electrospinning, fibers adhered the top load if the edge was not fixed. It took about 274 s to completely detach the web from the top load (Videos S1 and S2). This substantial expansion of fibrous structure caused damage of fiber web and faulty of the fibrous device. For the interconnected fiber web produced by short-distance electrospinning, however, it firmly attached one side without expansion, indicating the excellent structure stability.

Figure 5a shows the delamination resistance of the PVDF fiber webs (see the measurement setup in the inset). The two

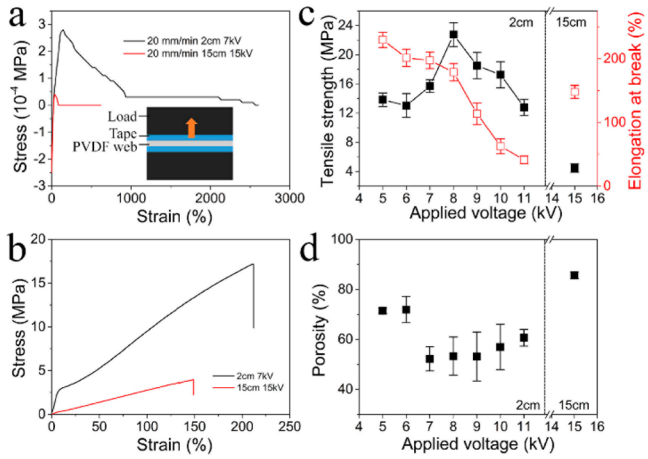

Figure 5. (a) Delamination resistance of the PVDF webs, (b) stress−strain curves of PVDF fiber webs, and effect of applied voltages on (c) tensile properties and (d) web porosity.

sides of the PVDF fiber web were mounted on the sample holders with double-side stick tape. For the interconnected fiber web, it required 280 Pa to delaminate the web when the cross-head speed was 20 mm/min, which was as strong as the sticking force between two layers of stick tapes (Figure S13). However, for the fiber web prepared by conventional electrospinning, the delamination strength was very small, only about 40 Pa.

We also measured the tensile property of the PVDF fiber webs, as seen in Figure 5b (also see Figures S14 and S15).

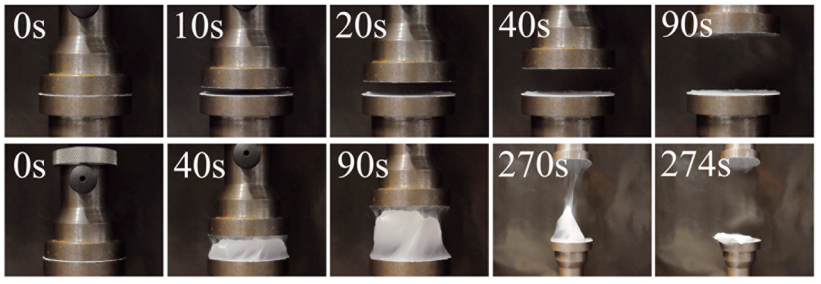

Figure 4. Digital photos of interconnected and separated fiber webs during the decompression.

DOI: 10.1021/acsami.5b06863
ACS Appl. Mater. Interfaces 2015, 7, 22551−22557

Before fracture, the fiber webs experienced two typical deformation stages: nonlinear deformation and linear elastic deformation.[27,28] The nonlinear elastic stage at the low stress comes from the guided alignment of randomly oriented fibers in the web. At the second stage, the curves showed a linear elasticity as the intrinsic property of aligned PVDF fibers.[29]

Figure 5c shows tensile properties of interconnected fiber webs prepared by short-distance electrospinning at the spinning distance of 2 cm. The web obtained at 5 kV had tensile strength and elongation at break of 13.82 MPa and 229.5%, respectively. When the applied voltage was increased to 6 kV, the tensile strength and elongation at break both decreased to 13.01 MPa and 201.22%. Increasing the voltage to 8 kV, the elongation at break decreased to 178.75% while the tensile strength increased to 22.75 MPa. When the applied voltage increased from 8 to 11 kV, both tensile strength and elongation at break decreased. Also, the webs looked like a transparent film that were very brittle and a plateau stage in the stress−strain curves appeared (Figure S14). The stress−strain curve of PVDF nanofiber web prepared by conventional electrospinning is also shown in Figure 5b,c. The higher tensile strength was attributed to denser fibrous structure. As shown in Figure 5d, the interconnected fiber webs had lower porosity than conventional PVDF nanofiber web.

The effect of spinning distances on tensile properties was also studied. It was indicated that interconnected fiber webs always had a higher tensile strength than separated fiber web (Figure S15).

Piezoelectric materials often undergo mechanical deformation during energy conversion. The active layer may receive forces from various directions (e.g., longitudinal or horizontal). The result that interconnected fiber webs obtained from short-distance electrospinning show evidently higher mechanical strength suggests that the interconnected fiber web should be more durable than that of the separated fiber web.

CONCLUSIONS

We have proven that interconnected PVDF fiber webs can be prepared by electrospinning a PVDF solution at a spinning distance of 2−8 cm. Most of the interconnected fibers have higher crystallinity than those prepared by conventional electrospinning, and the highest β phase content is comparable to that of the conventionally electrospun PVDF nanofibers. At the optimized condition, interconnected PVDF fiber web shows comparable mechanical-to-electrical conversion performance than the conventionally electrospun PVDF nanofiber web. However, interconnected fiber webs have higher delamination resistance and tensile strength. The higher mechanical strength allows the interconnected fiber web more robust to maintain structure integrity during compression and decompression. This makes interconnected PVDF fiber webs very promising for the development of mechanical energy harvesters.

ASSOCIATED CONTENT

Supporting Information

The Supporting Information is available free of charge on the ACS Publications website at DOI: 10.1021/acsami.5b06863.

SEM, DSC, XRD, FTIR, piezoelectric output signals, and mechanical property of fiber webs. β phase content calculation and crystallinity calculation. (PDF)

Video of decompression process of interconnected fiber webs. (AVI)

Video of decompression process of separated fiber webs. (AVI)

AUTHOR INFORMATION

Corresponding Author

*Tel.: +61 3 5227 1245. E-mail: tong.lin@deakin.edu.au.

Notes

The authors declare no competing financial interest.

ACKNOWLEDGMENTS

The authors acknowledge the support from Australian Research Council (ARC) through a Future Fellowship grant (ARC FT120100135) and a discovery grant (DP140100079).

REFERENCES

(1) Pradel, K. C.; Wu, W.; Ding, Y.; Wang, Z. L. Solution-Derived ZnO Homojunction Nanowire Films on Wearable Substrates for Energy Conversion and Self-Powered Gesture Recognition. *Nano Lett.* **2014**, *14*, 6897−6905.

(2) Xu, S.; Hansen, B. J.; Wang, Z. L. Piezoelectric-Nanowire-Enabled Power Source for Driving Wireless Microelectronics. *Nat. Commun.* **2010**, *1*, 93.

(3) Qiu, Y.; Lei, J.; Yang, D.; Yin, B.; Zhang, H.; Bian, J.; Ji, J.; Liu, Y.; Zhao, Y.; Luo, Y. Enhanced Performance of Wearable Piezoelectric Nanogenerator Fabricated by Two-Step Hydrothermal Process. *Appl. Phys. Lett.* **2014**, *104*, 113903.

(4) Zhong, Q.; Zhong, J.; Hu, B.; Hu, Q.; Zhou, J.; Wang, Z. L. A Paper-Based Nanogenerator as a Power Source and Active Sensor. *Energy Environ. Sci.* **2013**, *6*, 1779−1784.

(5) Zhou, T.; Zhang, C.; Han, C. B.; Fan, F. R.; Tang, W.; Wang, Z. L. Woven Structured Triboelectric Nanogenerator for Wearable Devices. *ACS Appl. Mater. Interfaces* **2014**, *6*, 14695−14701.

(6) Mao, Y.; Zhao, P.; McConohy, G.; Yang, H.; Tong, Y.; Wang, X. Sponge-like Piezoelectric Polymer Films for Scalable and Integratable Nanogenerators and Self-Powered Electronic Systems. *Adv. Energy Mater.* **2014**, *4*.10.1002/aenm.201301624

(7) Matsushige, K.; Nagata, K.; Imada, S.; Takemura, T. The II-I Crystal Transformation of Poly(vinylidene fluoride) under Tensile and Compressional Stresses. *Polymer* **1980**, *21*, 1391−1397.

(8) Lee, C.; Tarbutton, J. A. Electric Poling-Assisted Additive Manufacturing Process for PVDF Polymer-Based Piezoelectric Device Applications. *Smart Mater. Struct.* **2014**, *23*, 095044.

(9) Fang, J.; Wang, X.; Lin, T. Electrical Power Generator from Randomly Oriented Electrospun Poly (vinylidene fluoride) Nanofibre Membranes. *J. Mater. Chem.* **2011**, *21*, 11088−11091.

(10) Mandal, D.; Yoon, S.; Kim, K. J. Origin of Piezoelectricity in an Electrospun Poly (vinylidene fluoride-trifluoroethylene) Nanofiber Web-Based Nanogenerator and Nano-Pressure Sensor. *Macromol. Rapid Commun.* **2011**, *32*, 831−837.

(11) Fang, J.; Niu, H.; Wang, H.; Wang, X.; Lin, T. Enhanced Mechanical Energy Harvesting Using Needleless Electrospun Poly (vinylidene fluoride) Nanofibre Webs. *Energy Environ. Sci.* **2013**, *6*, 2196−2202.

(12) Shao, H.; Fang, J.; Wang, H.; Lin, T. Effect of Electrospinning Parameters and Polymer Concentrations on Mechanical-to-electrical Energy Conversion of Randomly-Oriented Electrospun Poly-(vinylidene fluoride) Nanofiber Mats. *RSC Adv.* **2015**, *5*, 14345−14350.

(13) Cavaliere, S.; Subianto, S.; Savych, I.; Jones, D. J.; Rozière, J. Electrospinning: Designed Architectures for Energy Conversion and Storage Devices. *Energy Environ. Sci.* **2011**, *4*, 4761−4785.

(14) Zhu, Y.; Han, X.; Xu, Y.; Liu, Y.; Zheng, S.; Xu, K.; Hu, L.; Wang, C. Electrospun Sb/C Fibers for a Stable and Fast Sodium-Ion Battery Anode. *ACS Nano* **2013**, *7*, 6378−6386.

(15) Hwang, T. H.; Jung, D. S.; Kim, J.-S.; Kim, B. G.; Choi, J. W. One-Dimensional Carbon−Sulfur Composite Fibers for Na−S

DOI: 10.1021/acsami.5b06863
ACS Appl. Mater. Interfaces 2015, 7, 22551−22557

Rechargeable Batteries Operating at Room Temperature. *Nano Lett.* **2013**, *13*, 4532−4538.
(16) Liu, Z.; Pan, C.; Lin, L.; Huang, J.; Ou, Z. Direct-Write PVDF Nonwoven Fiber Fabric Energy Harvesters via the Hollow Cylindrical Near-field Electrospinning Process. *Smart Mater. Struct.* **2014**, *23*, 025003.
(17) Chang, C.; Tran, V. H.; Wang, J.; Fuh, Y.; Lin, L. Direct-Write Piezoelectric Polymeric Nanogenerator with High Energy Conversion Efficiency. *Nano Lett.* **2010**, *10*, 726−731.
(18) Hong, Y.; Shang, T.; Li, Y.; Wang, L.; Wang, C.; Chen, X.; Jing, X. Synthesis Using Electrospinning and Stabilization of Single Layer Macroporous Films and Fibrous Networks of Poly (vinyl alcohol). *J. Membr. Sci.* **2006**, *276*, 1−7.
(19) Yee, W. A.; Kotaki, M.; Liu, Y.; Lu, X. Morphology, Polymorphism Behavior and Molecular Orientation of Electrospun Poly (vinylidene fluoride) Fibers. *Polymer* **2007**, *48*, 512−521.
(20) Bock, N.; Woodruff, M. A.; Hutmacher, D. W.; Dargaville, T. R. Electrospraying, a Reproducible Method for Production of Polymeric Microspheres for Biomedical Applications. *Polymers* **2011**, *3*, 131−149.
(21) Liu, Y.; Li, Y.; Xu, J.; Fan, Z. Cooperative Effect of Electrospinning and Nanoclay on Formation of Polar Crystalline Phases in Poly (vinylidene fluoride). *ACS Appl. Mater. Interfaces* **2010**, *2*, 1759−1768.
(22) Bachmann, M.; Gordon, W.; Koenig, J.; Lando, J. An Infrared Study of Phase-III Poly(vinylidene fluoride). *J. Appl. Phys.* **1979**, *50*, 6106−6112.
(23) Yu, H.; Huang, T.; Lu, M.; Mao, M.; Zhang, Q.; Wang, H. Enhanced Power Output of an Electrospun PVDF/MWCNTs-Based Nanogenerator by Tuning its Conductivity. *Nanotechnology* **2013**, *24*, 405401.
(24) Martins, P.; Lopes, A.; Lanceros-Mendez, S. Electroactive Phases of Poly (vinylidene fluoride): Determination, Processing and Applications. *Prog. Polym. Sci.* **2014**, *39*, 683−706.
(25) Zhao, S.; Wu, X.; Wang, L.; Huang, Y. Electrospinning of Ethyl−cyanoethyl cellulose/Tetrahydrofuran Solutions. *J. Appl. Polym. Sci.* **2004**, *91*, 242−246.
(26) Ero-Phillips, O.; Jenkins, M.; Stamboulis, A. Tailoring Crystallinity of Electrospun PLLA Fibres by Control of Electrospinning Parameters. *Polymers* **2012**, *4*, 1331−1348.
(27) Zhai, Y.; Wang, N.; Mao, X.; Si, Y.; Yu, J.; Al-Deyab, S. S.; El-Newehy, M.; Ding, B. Sandwich-Structured PVdF/PMIA/PVdF Nanofibrous Separators with Robust Mechanical Strength and Thermal Stability for Lithium Ion Batteries. *J. Mater. Chem. A* **2014**, *2*, 14511−14518.
(28) Wang, X.; Si, Y.; Wang, X.; Yang, J.; Ding, B.; Chen, L.; Hu, Z.; Yu, J. Tuning Hierarchically Aligned Structures for High-Strength PMIA−MWCNT Hybrid Nanofibers. *Nanoscale* **2013**, *5*, 886−889.
(29) Zhou, Y.; Fang, J.; Wang, X.; Lin, T. Strip Twisted Electrospun Nanofiber Yarns: Structural Effects on Tensile Properties. *J. Mater. Res.* **2012**, *27*, 537−544.

DOI: 10.1021/acsami.5b06863
ACS Appl. Mater. Interfaces 2015, 7, 22551−22557